Computers and Concrete, *Vol. 16, No. 6 (2015) 919-932*
DOI: http://dx.doi.org/10.12989/cac.2015.16.6.919

Non-destructive assessment of the three-point-bending strength of mortar beams using radial basis function neural networks

Alex Alexandridis*, Ilias Stavrakas, Charalampos Stergiopoulos, George Hloupis, Konstantinos Ninos and Dimos Triantis

Department of Electronic Engineering, Technological Educational Institute of Athens, Ag. Spiridonos, 12210, Aigaleo, Athens,Greece

(Received May 6, 2015, Revised November 25, 2015, Accepted December 14, 2015)

Abstract. This paper presents a new method for assessing the three-point-bending (3PB) strength of mortar beams in a non-destructive manner, based on neural network (NN) models. The models are based on the radial basis function (RBF) architecture and the fuzzy means algorithm is employed for training, in order to boost the prediction accuracy. Data for training the models were collected based on a series of experiments, where the cement mortar beams were subjected to various bending mechanical loads and the resulting pressure stimulated currents (PSCs) were recorded. The input variables to the NN models were then calculated by describing the PSC relaxation process through a generalization of Boltzmannn-Gibbs statistical physics, known as non-extensive statistical physics (NESP). The NN predictions were evaluated using k-fold cross-validation and new data that were kept independent from training; it can be seen that the proposed method can successfully form the basis of a non-destructive tool for assessing the bending strength. A comparison with a different NN architecture confirms the superiority of the proposed approach.

Keywords: non-destructive testing; three-point-bending strength; Pressure Stimulated Currents; non-extensive statistical physics; neural networks; radial basis function; fuzzy means

1. Introduction

The structural behaviour of cement based constructions is affected due to various factors like heavy loads, fatigue, aging and natural disasters. Thus, the investigation of the mechanical status of such constructions is of high interest to ensure the infrastructures safety conditions. Under this concept, diagnostic methods for the assessment of the mechanical status are continuously developed aiming at a real time monitoring of the structural health. Such methods include crack opening sensors attached on the buildings, accelerometers etc. These methods are mainly used for the monitoring of surface damages, a fact that limits the internal damage investigation and assessment. Recently, testing methods both destructive and non-destructive have been introduced

*Corresponding author, Associate Professor, E-mail: alexx@teiath.gr

http://www.techno-press.org/?journal=cac&subpage=8 ISSN: 1598-8198 (Print), 1598-818X (Online)

for the evaluation of cement based materials and structures. Modern techniques mainly based on non-destructive testing have attracted the attention of scientists and engineers as they are able to provide flexibility regarding the mechanical health status of a specimen or structure in situ or in a laboratory (Balayssac *et al*. 2013). Non-destructive testing techniques infer the internal damage, based on measurements that do not require destroying the material. However, a model is needed to produce a correlation between such measurements and the material status.

Neural networks (NNs) (Haykin 1999) offer a successful alternative for producing black box models without using a priori information about the system. Due to their ability to approximate successfully nonlinear and complex relationships based solely on input-output data, NNs constitute good candidates for producing non-destructive testing correlations. In fact, NNs have been used extensively in the non-destructive testing of concrete. Hybrid multilayer perceptron (HMLP) networks have been used by Tsai (2010) to predict strength of concrete-type specimens. NN models have been developed by Demir (2015) in order to predict the compressive and bending strengths of hybrid fibre-added concretes. The strength of of high-performance concrete has been modelled using NNs by Yeh (1998). NN and multiple linear regression (MLR) models have been used to determine the compressive strength of clinker mortars (Beycioğlu *et al*. 2015).

Radial basis function (RBF) networks (Alexandridis *et al*. 2012b) form an important network architecture with many advantages over other NN types including better approximation capabilities, simpler network structures and faster learning algorithms. As far as the latter are concerned, the fuzzy means (FM) algorithm (Sarimveis *et al*. 2002, Alexandridis *et al*. 2003) is an innovative approach with important merits, including automatic determination of the size of the network, i.e. the number of hidden nodes, and fast computational times and has found many applications in diverse fields including biomedical systems (Alexandridis and Chondrodima 2014), automatic control systems (Alexandridis *et al*. 2013), soft-sensors (Alexandridis 2013). etc. The algorithm was recently hybridized with the particle swarm optimization (PSO) method to further enhance its prediction capabilities (Alexandridis *et al*. 2012b).

In order to apply similar methods based on black-box modelling, it is important to define a suitable set of parameters to use as inputs to the NN. One of the testing methods that is under laboratory study deals with the recording of weak electric signals that are detected when natural building materials (i.e. marble, amphibolite etc) or artificial building materials (i.e. cement based, like cement paste, mortar etc) are subjected to mechanical loading. The detection of these electrical signals (weak electrical current emissions), is conducted through a novel experimental technique that is known under the term Pressure Stimulated Currents Technique and the recorded electrical signals are known as Pressure Stimulated Currents (PSC) (Stavrakas *et al*. 2004). The term Pressure Stimulated Currents has first been referred in the literature in order to describe the emission of a transient (polarization or depolarization) electrical signal, as a result of a gradual variation of the pressure on a solid containing electric dipoles due to defects (Varotsos *et al*. 1982 Varotsos and Alexopoulos 1984, Varotsos and Alexopoulos 1986, Varotsos *et al*. 1998).

The PSC signals provide important information about the damage processes occurring in the bulk of the specimen under test. Thus, the PSC experimental technique has been adopted for various loading modes in order to evaluate its applicability for a wide range of applications. Specifically, the used specimens were subjected to compressive stress (Stavrakas *et al*. 2004, Triantis *et al*. 2006, Triantis *et al*. 2007, Kyriazopoulos *et al*. 2011a, Triantis *et al*. 2012), and Three Point Bending (3PB) loading (Kyriazopoulos *et al*. 2011a). Noticeable PSC recordings have been reported when marble (Kyriazis *et al*. 2006) and cement based (Kyriazopoulos *et al*., 2011a) specimens are subjected to abrupt changes of mechanical loads up to specific load level and

consequently the load is maintained constant. During such load changes the PSC shows a spike-like behaviour while its relaxation back to the background level provides significant information regarding the mechanical status of the specimen. In previous works the PSC relaxation process was attempted to be described by an empirical equation described by two exponential decays (Triantis *et al*. 2007, Kyriazopoulos *et al*. 2011a, Kyriazopoulos *et al*. 2011b, Kyriazis *et al*. 2006, Kyriazis *et al*. 2009). In this work the main query that deals with the physical properties of the PSC relaxation process and the law that it follows until its relaxation back to its background level is discussed under the frame of statistical physics and specifically the Tsallis entropy. PSCs in stressed materials are produced by microfracture creation and evolution mechanisms (Enomoto and Hashimoto 1990, O'Keefee and Thiel 1995, Vallianatos *et al*. 2004, Stavrakas *et al*. 2004, Hadjicontis and Mavromatou 1994). These mechanisms are the roots of disorder and long range interactions and thus a generalization of the Boltzmannn-Gibbs (BG) statistical physics known as non-extensive statistical physics (NESP) (Tsallis 2009, Tsallis 1999, Vallianatos 2013, Sarlis *et al*. 2010), could be the theoretical ground for their analysis.

According to NESP, the entropy is not additive (Tsallis 2009, Vallianatos 2013), due to the fact, that is not proportional to the number of the system's elements in contrary to the *BG* entropy S_{BG}. Specifically, according to Tsallis the entropy S_q is defined as (Tsallis 2009)

$$S_q = k_B \frac{1-\sum_{i=1}^{W} p_i^q}{q-1} \tag{1}$$

where k_B is Boltzmann's constant, p_i is a set of probabilities, W is the total number of microscopic configurations, and q the entropic index. The entropic index q may be used to quantify the non-additivity of the studied physical system that accounts for the case of many non-independent, long-range interacting subsystems and memory effects (Tsallis 2009, Tsallis 1999, Vallianatos 2013). Detailed discussion on the physical interpretation of the Tsalis parameters that are used in this work may be found in previous works (Stergiopoulos *et al*. 2015).

A main target is to provide a decision system regarding the estimation of the mechanical status of a specimen. This, was primarily conducted in a previous publication (Alexandridis *et al*. 2012a), when cement based specimens were subjected to low level compressional stress. A series of laboratory experiments have been conducted in order to record the PSC in cement mortar specimens. Selected signal characteristics were correlated with the ultimate compressive strength of each specimen through the use of a neural network, employing a special training algorithm that offers increased predictive abilities. Results showed that the ultimate compressive strength can be successfully predicted without destroying the specimen.

In this paper, we extend the work presented by Alexandridis *et al*. (2012a) by introducing an NN approach for assessing a different property of mortar beams, namely the three-point-bending strength. The NN input parameters are extracted using PSC signals; however, in contrast to Alexandridis *et al*. (2012a), in this work we use NESP analysis to calculate the characteristic values which will be given to the NN as inputs. The RBF architecture is used in conjunction with the FM algorithm, which has been found to produce models with increased accuracy.

The rest of this paper is structured as follows: In the second section, we describe the materials and experimental arrangement used to produce the mortar beams. Section 3 describes the experimental procedure used to collect the training data for the NN. The NN parameter analysis and calculation is presented in section 4. A brief introduction to RBF networks and the applied training algorithm, followed by the methods used for model selection and data splitting is given in

section 5. Section 6 presents the results of applying the proposed non-destructive testing technique and relative discussion. The paper concludes by outlining the advantages of the proposed approach and setting some directions for future research.

2. Materials and experimental arrangement

A cement mortar mixture was used to prepare identical specimens in order to conduct the 3PB tests. The mixture included cement, sand (fine aggregates) and water at weight ratio 1:3:0.5 respectively. Detailed description of the specimen preparation process may be found in previous works (Stergiopoulos *et al*. 2013). The dimensions of the specimens were 250 mm long with a square cross-section of 50 mm 50mm. For obtaining 95% of their total strength the specimens were used for experiments 90 days after their preparation (Kosmatka *et al*. 2002). Preliminary 3PB strength tests have shown that the fracture limit (L_f) of the produced specimens was 3.8kN up to 4.1 kN.

The basic experimental setup for measuring the PSC is shown in Fig. 1. The Instron DX-300 electromechanical loading system (300kN capacity) was used in load control mode to apply loads to the specimen at a rate of 100 N/s. Two identical rigid metallic cylindrical supporting rollers and one loading roller were used for performing the 3PB test. The distance of the supporting roller–specimen contact point from the center of the beam was 90mm. The loading is applied on a third roller at the top-middle zone of the specimen in order to achieve bending. The three points of bending were electrically isolated by using Teflon plates of 2 mm thickness.

The PSC was captured by the electrodes and measured using a high sensitivity electrometer (Keithley, model 6514). The PSC electrodes were placed at the lower side of the beam (tensional zone) and were attached at the left and right of the specimen's loading plane. This topology was decided after several experiments that were conducted in order to estimate the best installation that ensures the recording of strong PSCs and limits the electrical noise influence. The best electrode distance (ℓ) was also investigated and it was empirically found that for the specific type of stored experiments the distance should be 35 mm approximately. The data was recorded in real time and

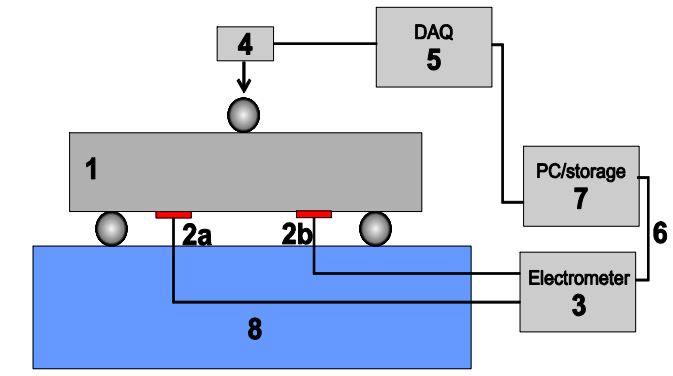

Fig. 1 The experimental arrangement and the selected location of the PSC electrodes (Sergiopoulos *et al*. 2015)

on a hard disk through a GPIB interface.The applied mechanical load was recorded with the using an analog-to-digital (A/D DAQ) data acquisition device (Keithley model KUSB-3108). The whole setup was placed in a Faraday shield in order to avoid interference from external electrical noise and the measurements remain unaffected. The details of the complete instrumentation set-up may be found in a previous work (Stergiopoulos *et al*. 2013).

3. Experimental procedure

A series of more than 60 cement mortar beams were subjected to 3PB tests according to the following loading pattern: Initially, a low mechanical load (L_0) of the order of 0.2kN, that is common for all the conducted experiments, is initially applied on the specimens in order to avoid possible parasitic initial effects caused either by friction or minor movements of the installation equipment. Sequentially, an abrupt mechanical load increase of high constant rate is applied on the mortar beam leading the specimen at a higher load value (L_h). The L_h load value is maintained on the cement mortar beam for a specific time period. The selected time period was 100s approximately in order to record the complete PSC relaxation process and at the same time to avoid the activation of any creep mechanisms (Stergiopoulos *et al*. 2015). For each of the conducted experiments a different level of L_h was selected and will be henceforth noticed as L_{hi}., where i i is the sequential experiment index number. Specifically, the applied L_{hi} level varied from relatively low values ($0.33L_f$) to significantly high values ($0.8L_f$) with respect to the ultimate 3PB strength (L_f) of the specimens.

The shape of the recorded PSC during the followed loading procedure is well deterministic and it is presented in previous works (Kyriazopoulos *et al*. 2011a, Kyriazis *et al*. 2009, Stergiopoulos *et al*. 2015). Specifically, the PSC obtains a spike-like shape reaching its peak value (I_0) at the moment (t_0) when the applied mechanical load reaches the level L_h and sequentially, while the applied load is maintained constant the PSC relaxes back to a background level (I_b). A generalized plot of the PSC behaviour is shown in Fig. 2.

4. Parameter analysis

In order to further analyze the experimental results non-extensive statistical physics were used based on Tsallis entropy. As reported earlier (Stergiopoulos *et al*. 2015) and since the studied system involves some multi-fractality it is expected that the PSC relaxation process follows an equation of the form

$$\frac{d\xi}{dt} = -\beta_q \cdot \xi^q \tag{2}$$

leading to the generalized q-exponential function (Vallianatos and Triantis 2013, Vallianatos *et al*. 2011, Christopoulos and Sarlis 2014)

$$\xi(t) = \exp_q(-(\frac{1}{\tau_q})\cdot t) = [1+(q-1)\cdot(\frac{1}{\tau_q})\cdot t]^{\frac{1}{1-q}} \tag{3}$$

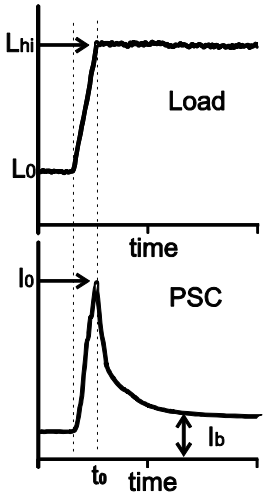

Fig. 2 A typical temporal recording of the PSC and the mechanical loading when the high rate step stress technique is applied (Sergiopoulos *et al*. 2015)

where $\xi(t)$ is the normalized PSC during the relaxation phase and may be calculated by using the following equation

$$\xi(t) = \frac{I(t) - I_b}{I_o - I_b} \tag{4}$$

where I_b is the value of the PSC background level and I_0 is the peak value of the PSC (see Fig. 2).

The entropic index q may be used to quantify the non-additivity of the studied physical system that accounts for the case of many non-independent, long-range interacting subsystems and memory effects (Tsallis, 2009, Tsallis, 1999). In most, if not all, of the studied applications, q appears to reflect some (multi) fractality in the system (Tsallis, 2009). τ_q is a parameter that reflects to a q-relaxation property.

As reported in previous works (Alexandridis *et al*. 2012a) a correlation between the electric charge Q and the damages in the bulk of a specimen exists. Thus, it was decided to attempt the use of the totally released electric charge during the application of an abrupt load increase as input for the designed NN. The electric charge Q was calculated during each loading step according to the following formulation

$$Q_i = \int_{t_0}^{t_1} PSC(t)dt \tag{5}$$

where t_0 is the time the mechanical load reaches its maximum value and t_1 the time the PSC relaxes back to the background level (i.e., 100s after reaching the load L_{hi})

5. Neural network models and non-destructive assessment

Neural networks have the ability to identify complex and nonlinear relationships based on

input-output data from an unknown system and therefore they could be used as tools for predicting critical properties of mortar beams in a non-destructive framework. During a training stage, the NN adapts its parameters so as to better approximate a subset of the available data, known as training data. The training task is usually formulated as an optimization problem, where the design variables are the network parameters and the objective function is a cost function, expressing the errors between the true outputs and the network predictions.

NNs can be assigned to different architectures, depending on the interconnection of the NN nodes and the calculations being performed inside each particular node. The following section gives a brief presentation of the RBF network architecture and the training algorithm used in this work.

5.1 RBF networks and the FM algorithm

An RBF network consists three different layers of nodes, namely the input, hidden and output layer. The input layer has the same dimensionality N with the input space and performs no calculations but only distributes the input variables to the hidden layer. The latter comprises of L computational nodes; each node is characterized by a center vector $\hat{\mathbf{x}}_l^T = [\hat{x}_{l,1}, \hat{x}_{l,2}, ..., \hat{x}_{l,N}]$. The activity $v_l(\mathbf{x}_k)$ of the l^{th} node is calculated as the Euclidean norm of the difference between the k^{th} input vector and the respective center and is given by

$$v_l(\mathbf{x}_k) = \left\| \mathbf{x}_k - \hat{\mathbf{x}}_l \right\| = \sqrt{\sum_{i=1}^{N} (x_{k,i} - \hat{x}_{l,i})^2} \quad , \qquad k = 1, 2, \ldots, K \tag{6}$$

where K is the number of training data, and $\mathbf{x}_k^T = [x_{k,1}, x_{k,2}, \ldots, x_{k,N}]$ is the input vector.

The result of this calculation is given as input to a function with radial symmetry. In this work, we use the thin-plate-spline function

$$g(v_l) = v_l^2 \log(v_l) \tag{7}$$

The output of each hidden node l is multiplied by a synaptic weight w_l and the final output for the k^{th} data point $\hat{y}_k$ is produced as a linear combination of the weighted hidden node responses

$$\hat{y}_k = \sum_{l=1}^{L} w_l g\left(v_l\left(\mathbf{x}_k\right)\right), \; k = 1, 2, \ldots, K \tag{8}$$

Usually, the training procedure for an RBF network is split in two distinct phases: a) calculation of the hidden layer node centers $\hat{\mathbf{x}}_l$ and b) calculation of the synaptic weights. The first stage, which is usually the most difficult one, can be implemented through unsupervised clustering methods, e.g., the k-means algorithm. Alternatively, an innovative approach known as the fuzzy means (FM) algorithm (Sarimveis *et al*. 2002, Alexandridis *et al*. 2003) can be applied to the selection of the hidden layer nodes. A brief description of the algorithm is given below; more details can be found in the original publications.

Consider a system with N normalized input variables u_i, where i=1, …,N. The domain of each input variable is partitioned into an equal number of one-dimensional triangular fuzzy sets, c. Each fuzzy set can be written as

$$A_{i,j} = \left\{ a_{i,j}, \delta\alpha \right\}, \quad i=1,\ldots,N, \quad j=1, \ldots, c. \tag{9}$$

where $a_{i,j}$ is the center element of fuzzy set $A_{i,j}$ and $\delta\alpha$ is half of the respective width. This partitioning technique creates a total of c^N multi-dimensional fuzzy subspaces $\mathbf{A}^l$, where l=1, …,c^N. The multi-dimensional fuzzy subspaces are generated by combining N one-dimensional fuzzy sets, one for each input direction.

Each one of the produced fuzzy subspaces is a candidate for becoming an RBF center, but only a subset of them will be finally selected, depending on the distribution of data within the input space. The selection is based on the idea of the multidimensional membership function $\mu_{\mathbf{A}^l}(\mathbf{x}_k)$ of an input vector $\mathbf{x}_k$ to a fuzzy subspace $\mathbf{A}^l$ which is given by Nie (1997)

$$\mu_{\mathbf{A}^l}(\mathbf{x}_k) = \begin{cases} 1 - r_l(\mathbf{x}_k), & \text{if } r_l(\mathbf{x}_k) \le 1 \\ & \\ 0 & \text{, otherwise} \end{cases} \quad , k = 1, 2, \ldots, K \tag{10}$$

where $r_l(\mathbf{x}_k)$ is the Euclidean relative distance between $\mathbf{A}^l$ and the input data vector $\mathbf{x}_k$

$$r_l(\mathbf{x}_k) = \sqrt{\sum_{i=1}^{N}\left(a_{i,j_i}^l - x_{i,k}\right)^2} \Big/ \delta a\sqrt{N} \tag{11}$$

Eq. (11) defines a hyper-sphere on the input space with radius equal to $\delta\alpha\sqrt{N}$. The objective of the training algorithm is to select a subset of fuzzy subspaces as RBF centers, so that all the training data are covered by at least one hyper-sphere. Expressing this requirement in terms of Eq. (11), the subset of fuzzy subspaces is selected so that there is at least one fuzzy subspace that assigns a nonzero multidimensional degree to each input training vector. The maximum possible number of selected RBF centers is equal to the number of training data, although, depending on the distribution of data in the input space, a smaller number of centers is usually produced.

Following the determination of centers by the fuzzy means algorithm, the synaptic weights are calculated using linear regression of the hidden layer outputs to the real measured outputs (target values). The regression problem can be trivially solved using linear least squares in matrix form via the following equation

$$\mathbf{W}^T = \mathbf{Y}^T \cdot \mathbf{Z} \cdot \left(\mathbf{Z}^T \cdot \mathbf{Z}\right)^{-1} \tag{12}$$

where $\boldsymbol{Z}$ contains the outputs of the hidden layer nodes and $\boldsymbol{Y}$ the target values.

5.2 k-fold cross validation for model selection

The training stage is usually followed by a model selection phase, where the objective is to select the number of hidden nodes. Usually a large number of hidden nodes produces lower errors as far as the training data are concerned. On the other hand, such a selection leads to overfitting, i.e. excessively fitting the model to the training data; this reduces the generalization ability of the model, as the network ends up in learning the noise that is present in the training data and its ability to model new, different data points is severely impaired. Successful completion of the training phase means that the NN model should be capable of producing accurate estimations of the output variables given a new set of input data.

In order to avoid the overfitting phenomenon, a technique known as *k*-fold cross-validation is

used for model selection. According to this method, the available data are split into *k* mutually exclusive subsets, known as folds. For each fold *k*, the network is trained using all folds except from *k*. The resulting model is then used to obtain predictions for all the datapoints belonging to the fold that was left out. This procedure is repeated *k* times, each time leaving a different fold out for obtaining predictions and the rest of the folds for training. Usually 10 folds are applied, a number which was also adopted in this study. When the *k*-fold method is completed, a prediction $\hat{y}_i$ for each datapoint is available, where datapoint *i* has not been used for training the model. Evaluation and model selection can then be performed using different error metrics. In this work, the root mean square error (RMSE) and the coefficient of determination R^2 are used. These two coefficients can be calculated as follows

$$\mathrm{RMSE} = \sqrt{\frac{\sum_{i=1}^{K}\left(\hat{y}_i - y_i\right)^2}{K}} \tag{13}$$

$$\begin{aligned} R^2 &= 1 - \frac{SS_{err}}{SS_{tot}} \\ SS_{err} &= \sum_{i=1}^{K}\left(y_i - \hat{y}_i\right)^2 \\ SS_{tot} &= \sum_{i=1}^{K}\left(y_i - \bar{y}\right)^2 \end{aligned} \tag{14}$$

In the above equation, $\bar{y}$ stands for the mean value of the output variable. Both RMSE and R^2 can be used as indicators for selecting the most appropriate model, which in this case means selecting the appropriate network size, and for evaluating the network performance.

5.3 Variable selection, data splitting and training

Training an NN model suitably in order to be used as a tool for non-destructive assessment initially requires the selection of proper input variables. In this work a set of parameters based on the PSC measurements and non-extensive statistical physics are used, namely the entropic index *q*, the *q*-relaxation property τ_q, the PSC background level I_b and the electric charge Q. Additionally, we feed the NN with the mechanical load value L_h , as different values were used per specimen.

A total of 67 datapoints were available, where each datapoint includes measurements for the 5 aforementioned variables to be used as inputs, together with the measured ultimate 3PB strength of the specimens L_f, which denotes the output variable of the network. Out of the 67 datapoints, 60 were used in the 10-fold cross validation procedure in order to train and select the best RBF network model as described in the previous section. The remaining 7 datapoints, which did not take any part whatsoever in the training and model selection procedures, were used for final evaluation and testing of the model. Testing the resulting model in a new set of data is crucial in

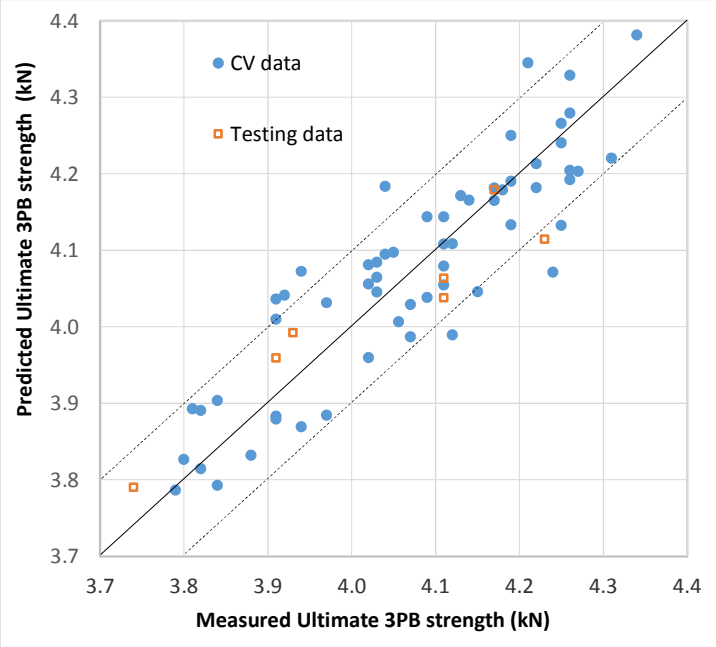

Fig. 3 Measured ultimate 3PB strength versus RBF network predictions. The black line corresponds to perfect fitting and the dashed lines correspond to ±0.1 kN modelling error

order to assess its true performance, as the model could have been overfitted in the training data even through the cross-validation procedure (Rao *et al*. 2008).

In order to train the RBF network, the FM algorithm was applied, testing in each cross-validation cycle all possible RBF networks with fuzzy partitions ranging from 4 to 30 fuzzy sets. The fuzzy partition producing the best R^2 in the cross-validation data was selected and used to obtain predictions for the testing data.

6. Results and discussion

Results of the RBF network training procedure are summarized in Table 1, where the RMSE and R^2 pointers are depicted for the data used for cross-validation and the testing data separately, together with the selected number of fuzzy sets and the resulting number of RBF centers. In order to compare results with a different NN implementation, feedforward neural networks (FFNN) trained with the Levenberg-Marquardt algorithm (Hagan and Menhaj 1994) were also tested. To be more specific, two-layered networks were used, and the number of nodes per layer was selected based on an exhaustive search procedure, testing all possible combinations in the range 5-30 nodes.

Fig. 3 gives a schematic overview of the ultimate 3PB strength measurements versus the predictions casted by the RBF network that produced the best results as far as the cross-validated data were concerned. Results for the testing data, which were excluded from the *k*-fold cross validation method and were kept completely independent from training, are also included in the same figure.

Table 1 Results for the RBF network training procedure and comparison with FFNN

	RBFNN	FFNN
Cross-validation RMSE (kN)	0.07	0.12
Cross-validation R^2	0.76	0.70
Cross-validation maximum error (kN)	0.17	0.21
Testing RMSE (kN)	0.07	0.09
Testing R^2	0.83	0.77
Testing maximum error (kN)	0.12	0.14
# of hidden nodes	18	[12 8] *
# of fuzzy sets	18	-

*For FFNNs the number of hidden nodes is given in the form (1st layer nodes 2nd layer nodes)

The plotted results, together with the values of the statistical pointers RMSE and R^2 indicate good modelling performance for the RBF-based predictor. This is also confirmed by the maximum errors generated by the RBF model, which remain relatively low. It should be noted that the RBF model performs satisfactory not only on the cross-validation data, but also on new testing data that have not been used at all in any stage of the training and model selection procedures. Based on the above, the RBF model could be used to successfully predict the ultimate 3PB strength measurements in a non-destructive manner, based only on the PSC readings. Finally it is important to note that based on the statistical indicators, the RBF model performance is clearly superior compared to the FFNN, in terms of higher prediction accuracy. This result could be attributed to the training approach followed in the case of RBF networks: calculation of the synaptic weights using linear regression guarantees a global minimum, while the FM algorithm provides a good selection of RBF centers. The superiority of RBF networks over FFNNs has been also confirmed by other researchers (Park *et al*. 2002)

7. Conclusions

This work presents a new method for predicting the 3PB strength of mortar beams using NN models. Assessment of the 3PB strength is performed in a completely non-destructive way, by measuring pressure stimulated currents generated by subjecting the specimens to low mechanical stress. Non-extensive statistical physics based on Tsallis entropy are used to extract meaningful features which are fed as input to an RBF network. The network is trained with the FM algorithm, which presents certain remarkable advantages, including increased prediction accuracy. A 10-fold cross validation procedure is used for model selection, while a small portion of the data is excluded from this procedure and kept for testing the produced model. Results show that the proposed approach can be used successfully for assessing the 3PB strength, whereas it outperforms a different NN training technique.

Acknowledgments

This research has been co-financed by the European Union (European Social Fund—ESF) (no.

MIS 379389) and Greek national funds through the Operational Program "Education and Lifelong Learning" of the National Strategic Reference Framework (NSRF)-Research Funding Program: ARCHIMEDES III. Investing in knowledge society through the European Social Fund.

References

Alexandridis, A., Sarimveis, H. and Bafas, G. (2003), "A new algorithm for online structure and parameter adaptation of RBF networks", *Neural Networks*, **16**(7), 1003-1017.

Alexandridis, A., Triantis, D., Stavrakas, I. and Stergiopoulos, C. (2012a), "A neural network approach for compressive strength prediction in cement-based materials through the study of pressure stimulated electrical signals", *Constr. Build. Mater.*, **30,** 294-300.

Alexandridis, A., Chondrodima, E. and Sarimveis, H. (2012b), "Radial basis function network training using a nonsymmetric partition of the input space and particle swarm optimization", *IEEE Trans. Neural Network. Learn. Syst.*, **24**(2), 219-230.

Alexandridis, A., Stogiannos, M. Kyriou, A. and Sarimveis, H. (2013), "An offset-free neural controller based on approximating the inverse process dynamics", *J. Process Cont.*, **23**(7), 968-979.

Alexandridis, A. (2013), "Evolving RBF neural networks for adaptive soft-sensor design", *Int. J. Neur. Syst.*, **23**(6), 1350029.

Alexandridis, A. and Chondrodima, E. (2014), "A medical diagnostic tool based on radial basis function classifiers and evolutionary simulated annealing", *J. Biomed. Inform.*, **49**, 61-72.

Balayssac, J.P., Laurens, S., Breysse, D. and Garnier, V. (2013), *Evaluation of concrete properties by combining NDT methods. Nondestructive Testing of Materials and Structures*, Springer, Netherlands.

Beycioğlu, A., Emiroğlu, M., Kocak, Y. and Subaş, S. (2015), "Analyzing the compressive strength of clinker mortars using approximate reasoning approaches-ANN vs MLR", *Comput. Concrete*, **15**(1), 89-102.

Christopoulos, S.R.G. and Sarlis, N.V. (2014), "q-exponential relaxation of the expected avalanche size in the coherent noise model", *Physica A: Stat. Mech. Appl.*, **407**, 216-225.

Demir, A. (2015), "Prediction of hybrid fibre-added concrete strength using artificial neural networks", *Comput. Concrete*, **15**(4), 503-514.

Enomoto, J. and Hashimoto, H. (1990), "Emission of charged particles from indentation fracture of rocks", *Nature*, **346**(6285), 641-643.

Hadjicontis, V. and Mavromatou, C. (1994), "Transient electric signals prior to rock failure under uniaxial compression", *Geophys. Res. Lett.*, **21**(16), 1687-1690.

Hagan, M.T. and Menhaj, M. (1994), "Training feedforward networks with the Marquardt algorithm", *IEEE Trans. Neural Netw.*, **5**, 989-993.

Hagan, M.T. and Menhaj, M.B. (1994), "Training feedforward networks with the Marquardt algorithm,", *Neural Networks, IEEE Tran.*, **5**(6), 989-993.

Haykin, S. (1999), *Neural Networks: A Comprehensive Foundation*, 2nd Edition, Prentice Hall, Upper Saddle River, NJ.

Kosmatka, S., Kerkhoff, B. and Panarese, W. (2002), *Design and control of concrete mixtures*, 14th Edition, Portland Cement Association, Skokie Illinois USA.

Kyriazis, P., Anastasiadis, C., Triantis, D. and Vallianatos, F. (2006), "Wavelet analysis on pressure stimulated currents emitted by marble samples", *Nat. Hazard. Earth Syst. Sci.*, **6**(6), 889-894.

Kyriazis, P., Anastasiadis, C., Stavrakas, I., Triantis, D. and Stonham, J. (2009), "Modelling of electric signals stimulated by bending of rock beams", *Int. J. Microstruct. Mater. Prop.*, **4**(1), 5-18.

Kyriazopoulos, A., Anastasiadis, C., Triantis, D. and Brown, C.J. (2011a), "Non-destructive evaluation of cement-based materials from pressure-stimulated electrical emission-Preliminary results", *Constr. Build. Mater.*, **25**, 1980-1990.

Kyriazopoulos, A., Stavrakas, I., Anastasiadis, C. and Triantis, D. (2011b), "Study of weak electric current

emission on cement mortar under uniaxial compressional mechanical stress up to the vicinity of fracture", *J. Mech. Eng.*, **57**, 237-244.
Nie, J. (1997), "Fuzzy control of multivariable nonlinear servomechanisms with explicit decoupling Scheme", *IEEE Tran. Fuzzy Syst.*, **5**(2), 304-311.
O'Keefee, S.G. and Thiel, D.V. (1995), "A mechanism for the production of electromagnetic radiation during fracture of brittle materials", *Phys. Earth Planet. Inter.*, **89**(1), 127-135.
Park, J.W., Harley, R.G. and Venayagamoorthy, G.K. (2002), "Comparison of MLP and RBF neural networks using deviation signals for on-line identification of a synchronous generator", *Power Engineering Society Winter Meeting, 2002. IEEE*, **1**, 274-279.
Rao, B., Fung, G. and Rosales, R. (2008), "On the dangers of cross-validation. An experimental evaluation", *Proceedings of the SIAM International Conference on Data Mining*, Atlanta, GA, USA.
Sarimveis, H., Alexandridis, A., Tsekourasm G. and Bafas, G. (2002), "A fast and efficient algorithm for training radial basis function neural networks based on a fuzzy partition of the input space", *Ind. Eng. Chem. Res.*, **41**(4), 751-759.
Sarlis, N.V., Skordas, E.S. and Varotsos, P.A. (2010), "Nonextensivity and natural time: The case of seismicity", *Phys. Rev. E.*, **82**(2), 021110.
Stavrakas, I., Anastasiadis, C., Triantis, D. and Vallianatos, F. (2003). "Piezo stimulated currents in marble samples: precursory and concurrent-with-failure signals", *Nat. Hazard. Earth Syst.Sci.*, **3**(3-4), 243-247.
Stavrakas, I., Triantis, D., Agioutantis, Z., Maurigiannakis, S., Saltas, V., Vallianatos, F. and Clarke, M. (2004), *Pressure stimulated currents in rocks and their correlation with mechanical properties.*
Stergiopoulos, C., Stavrakas, I., Hloupis, G., Triantis, D. and Vallianatos, F. (2013), "Electrical and acoustic emissions in cement mortar beams subjected to mechanical loading up to fracture", *Eng. Fail. Anal.*, **35**, 454-461.
Stergiopoulos, C., Stavrakas, I., Triantis, D., Vallianatos, F. and Stonham, J. (2015), "Predicting fracture of mortar beams under three-point bending using non-extensive statistical modelling of electric emissions", *Physica A*, **419**, 603-611.
Triantis, D., Stavrakas, I., Anastasiadis, C., Kyriazopoulos, A. and Vallianatos, F. (2006), "An analysis of pressure stimulated currents (PSC), in marble samples under mechanical stress", *Phys. Chem. Earth, Parts A/B/C*, **31**(4), 234-239.
Triantis, D., Anastasiadis, C., Vallianatos, F., Kyriazis, P. and Nover, G. (2007), "Electric signal emissions during repeated abrupt uniaxial compressional stress steps in amphibolite from KTB drilling", *Nat. Hazard. Earth Syst. Sci.*, **7**, 149-154.
Triantis, D., Stavrakas, I., Kyriazopoulos, A., Hloupis, G. and Agioutantis, Z. (2012), "Pressure stimulated electrical emissions from cement mortar used as failure predictors", *Int. J. Fract.*, **175**(1), 53-61.
Tsai, H.C. (2010), "Predicting strengths of concrete-type specimens using hybrid multilayer perceptrons with center-unified particle swarm optimization", *Expert Syst. Appl.*, **37**(2), 1104-1112.
Tsallis, C. (1999), "Nonextensive statistics: theoretical, experimental and computational evidences and connections", *Braz. J. Phys.*, **29**(1), 1-35.
Tsallis, C. (2009), *Introduction To Nonextensive Statistical Mechanics: Approaching A Complex World*, Springer, Berlin.
Vallianatos, F., Triantis, D., Tzanis, A., Anastasiadis, C. and Stavrakas, I. (2004), "Electric earthquake precursors: from laboratory results to field observations", *Phys. Chem. Earth, Parts A/B/C*, **29**(4), 339-351.
Vallianatos, F., Triantis, D. and Sammonds, P. (2011), "Non-extensivity of the isothermal depolarization relaxation currents in uniaxial compressed rocks", *Europhys. Lett.*, **94**(6), 68008.
Vallianatos, F. (2013), "On the statistical physics of rockfalls: A non-extensive view", *Europhys. Lett.*, **101**(1), 10007.
Vallianatos, F. and Triantis, D. (2013), "A non-extensive view of the pressure stimulated current relaxation during repeated abrupt uniaxial load-unload in rock samples", *Europhys. Lett.*, **104**(6), 68002.
Varotsos, P., Alexopoulos, K. and Nomicos, K. (1982), "Comments on the pressure variation of the Gibbs energy for bound and unbound defects", *Physica Status Solidi B*, **111**(2), 581-590.

Varotsos, P. and Alexopoulos, K. (1984), "Physical properties of the variations of the electric field of the earth preceding earthquakes, II. Determination of epicenter and magnitude", *Tectonophysics*, **110**(1), 99-125. (see page 122)

Varotsos, P. and Alexopoulos, K. (1986), *Thermodynamics of point defects and their relation with the bulk properties*, Eds. S. Amelinckx, R. Gevers, and J. Nihoul, North Holland.

Varotsos, P., Sarlis, N., Lazaridou, M. and Kapiris, P. (1998), "Transmission of stress induced electric signals in dielectric media", *J. Appl. Phys.*, **83**(1), 60-70.

Yeh, I.C. (1998), "Modeling of strength of high-performance concrete using artificial neural networks", *Cement Concrete Res.*, **28**(12), 1797-1808.

CC